MAGNETIC ANALYSES OF NEW ANTARCTIC IRON METEORITES

Takesi NAGATA, Minoru FUNAKI

National Institute of Polar Research, 9–10, Kaga 1-chome, Itabashi-ku, Tokyo 173

and

Isamu TAGUCHI

R & D Laboratories-1, Nippon Steel Corporation, 1618, Ida, Nakahara-ku, Kawasaki 211

Abstract: Four new Antarctic iron meteorites collected at Yamato meteorite ice field in 1979, Yamato-790517, -790724, -791076 and -791694, are magnetically analyzed. Characteristics of their magnetic hysteresis curves and thermomagnetic curves indicate the following meteoritic structures of these iron meteorites.

Yamato-790517 is a Ni-poor ataxite consisting of kamacite matrix of 6.4 wt%Ni, unequilibrated Ni-rich kamacite specks of about 12 wt%Ni and taenite specks. Yamato-790724 is a coarse octahedrite of kamacite matrix of 7.0 wt%Ni and taenite specks. Yamato-791076 is a finest octahedrite or an ataxite which consists of kamacite of 7.3 wt%Ni and plessite of about 12 wt%Ni. Yamato-791694 is a Ni-rich ataxite consisting mostly of taenite of about 40 wt%Ni and a small amount of kamacite specks.

Two Antarctic iron meteorites collected near Allan Hills in Victoria Land in 1977, Allan Hills-77263 and -77289, also are magnetically analyzed. Both the iron meteorites are coarse octahedrites comprising kamacite matrix of about 6.5 wt%Ni and taenite specks.

1. Introduction

Early studies on magnetic properties of iron meteorites have been summarized by LOVERING and PARRY (1962) and by GUS'KOVA (1972). These early works demonstrated that the thermomagnetic characteristics of iron meteorites are generally the irreversible thermomagnetic curves of the b.c.c. α-phase (kamacite) of Fe-Ni metal and/or the reversible thermomagnetic curves of the f.c.c. γ-phase (taenite) of Fe-Ni metal. In particular, LOVERING and PARRY attempted to quantitatively identify the nickel content of coexisting kamacite, taenite and plessite ($\alpha + \gamma$ phase) in all major structure classes of iron meteorites such as hexahedrite, Ni-poor ataxite, octahedrite and Ni-rich ataxite. In addition to these major phases of iron meteorites, they magnetically detected iron-nickel phosphide, $(Fe, Ni)_3P$, such as schreibersite and rhabdite also in iron meteorites.

Chemical, metallographical and magnetic properties of several iron meteorites in the collection of new Antarctic meteorites have already been studied. They are Yamato-75105 Ni-poor ataxite (NAGATA *et al.*, 1976), Yamato-75031 Ni-rich ataxite (FISHER *et al.*, 1978; NAGATA, 1978), Allan Hills 762 octahedrite (FISHER *et al.*, 1979), Allan

Hills A77255 ataxite, Derrick Peak A78003 hexahedrite, and Derrick Peak A78007 octahedrite (FISHER *et al.*, 1980). In these Antarctic iron meteorites also, kamacite, plessite and taenite phases of Fe-Ni metals are the major components and lamellae or specks of Fe-Ni phosphide are present as the minor constituents.

Based on the magnetic characteristics of 16 iron meteorites represented by the magnetic hysteresis curves and the thermomagnetic curves of the Antarctic iron meteorites and those of iron meteorites magnetically examined by LOVERING and PARRY (1962), NAGATA (1982) has proposed a provisional scheme of magnetic classification of iron meteorites into three groups, *i.e.* a group of hexahedrite and Ni-poor ataxite, octahedrite group and Ni-rich ataxite group. In the proposed classification scheme, two magnetic parameters, namely, (a) a ratio of the saturation magnetization intensity of kamacite component, $I_s(\alpha)$, to that of the whole meteorite, I_s, *i.e.*, $I_s(\alpha)/I_s$, and (b) the transition temperature from γ-phase to α-phase of kamacite component on the cooling thermomagnetic curve ($\Theta^*_{\gamma \to \alpha}$) or Curie point temperature of taenite component (Θ_c) in case that only taenite component magnetization exists, are adopted for representing the magnetic characteristics of iron meteorites. In a two-dimensional rectangular coordinates diagram of $I_s(\alpha)/I_s$ *vs.* $\Theta^*_{\gamma \to \alpha}$ or Θ_c, hexahedrite plus Ni-poor ataxite, octahedrite and Ni-rich ataxite groups are well separately confined within their respective domains.

It seems however that the number and variety of iron meteorites whose magnetic properties are well analyzed with reference to their chemical and metallographical compositions are still too few at present to set up a general scheme of "iron meteorite magnetism". Up to the present time, four new iron meteorites have been discovered in the Meteorite Ice Field near Yamato Mountains in East Antarctica by Japanese Antarctic Research Expedition teams. They are Yamato-790517, -790724, -791076 and -791694. Descriptions of their chemical and metallographical composition in detail will be given in a separate paper. In the present note, representative magnetic properties of these four new Yamato iron meteorites will be described and discussed with reference to their major chemical and metallographical compositions. In addition, similar analyses and discussions will be made on two iron meteorites recovered from the ice-sheet surface near Allan Hills in Victoria Land in West Antarctica. The examined iron meteorites are Allan Hills-77263 and -77289.

2. Outline of Chemical and Metallographical Properties

The bulk chemical compositions of 6 Antarctic iron meteorites are measured by a computer-aided microanalyzer. The weight percentage of bulk contents of Ni, Co and P are summarized in Table 1. As the total of all other elements such as S, Ga, Ge, Ir and others is less than 0.1 wt%, we may approximately consider that the remainder after subtracting the contents of Ni, Co and P is almost identical to the Fe content. Judging from the bulk chemical composition, Yamato-790517 and -790724 and Allan Hills-77263 and -77289 are coarse octahedrites or Ni-poor ataxite, while Yamato-791076 is either finest octahedrite or Ni-rich ataxite and Yamato-791694 is a Ni-rich ataxite. Characteristic metallographical structures of individual iron meteorites are as follows:

Yamato-790517: Throughout this Ni-poor ataxite, fine granular grains of Ni-rich kamacite and Fe-Ni phosphide are dispersed in kamacite matrix of 7.0 wt%Ni.

Table 1. Bulk chemical composition of new Antarctic iron meteorites.

Iron Meteorite	Ni	Co (wt%)	P	q: Fe-Ni phosphide (wt%)
Yamato-790517	7.42	0.58	0.41	—
Yamato-790724	7.46	0.47	0.12	0.04
Yamato-791076	13.60	0.76	0.28	1.57
Yamato-791694	35.50	0.60	0.15	0.89
Allan Hills-77263	6.78	0.47	0.20	0.71
Allan Hills-77289	6.79	0.52	0.18	0.67

The grain size of Ni-rich kamacite component ranges from 5 to 15 μm in mean diameter, while the mean diameter of Fe-Ni phosphide grains from 10 to 30 μm. The chemical compositions of the Ni-rich kamacite grains are approximately given by (18–24) wt%Ni, (0.4±0.1) wt%Co and (0.3±0.1) wt%P, while the Fe-Ni phosphide grains are chemically separated into two groups, namely, a group of (10–16) wt%Ni, (0.54±0.02) wt%Co and (0.75±0.20) wt%P and the other group of (10–16) wt%Ni, (0.57±0.04) wt%Co and (5–10) wt%P. As given in Table 1, the bulk content of P in Yamato-790517 is the largest (0.41 wt%P) among the six iron meteorites examined in the present study. Since the chemical composition of kamacite matrix is given by (6.97±0.10) wt%Ni, (0.68±0.01) wt%Co and (0.24±0.02) wt%P, the excess amount of P may tend to form Fe-Ni phosphide. However the P-contents in the Fe-Ni phosphide grains in Yamato-790517 are too small to form schereibersite structures, $(Fe, Ni)_3P$.

Yamato-790724: As described in a previous paper (NAGATA *et al.*, 1983), lamellae and fine specks of Fe-Ni phosphide and taenite are dispersed in kamacite matrix of this coarse octahedrite. Further analyses have shown that the chemical composition of kamacite matrix is given by (7.00±0.03) wt%Ni, (0.45±0.01) wt%Co and (0.11±0.01) wt%P, and that of taenite by (28.0–33.0) wt%Ni, 0.12 wt%Co and 0.02 wt%P. The composition of Fe-Ni phosphide is given by 54.84 wt%Fe, 29.06 wt%Ni, 0.12 wt%Co and 15.97 wt%P.

Yamato-791076: As the bulk Ni content in this iron meteorite is 13.60 wt%, its metallographic structure is in-between that of finest octahedrite and that of Ni-rich ataxite. The major parts of Yamato-791076 are covered by microplessitic net systems consisting of taenite net-frames of 21.5–36.5 wt%Ni, where the size of taenite net-meshes is 3×10 μm in the order of magnitude, kamacite of 5.1 wt%Ni fulfilling the net-mesh space. Spindle-shape gaps of 40–80 μm in width between neighboring individual microplessitic nets also are occupied by kamacite of 7.0 wt%Ni. The kamacite spindles include Fe-Ni phosphide specks of chemical composition of 42.7 wt%Fe, 41.5 wt%Ni and 15.6 wt%P.

Yamato-791694: As suggested by the bulk chemical composition represented by 35.50 wt%Ni, this iron meteorite is a Ni-rich ataxite, the matrix of which is either homogeneous taenite of (64.0±0.4) wt%Fe, (35.5±0.4) wt%Ni and (0.68±0.02) wt%Co, or taenite matrix of a similar chemical compostion including dispersed kamacite specks of 6.8 wt%Ni and 1.8 wt%Co. This Ni-rich ataxite also contains Fe-Ni phosphide specks of (41.8±0.5) wt%Fe, (43.3±0.7) wt%Ni, (0.32±0.01) wt%Co and

(15.8±0.1) wt%P. The edge surface layer of these Fe-Ni phosphide specks is kamacite of 6.7 wt%Ni and 1.7 wt%Co.

Allan Hills-77263: As already reported (NAGATA *et al.*, 1983), Allan Hills-77263 coarse octahedrite contains thin lamellae (30–50 μm in width) of taenite (34.8 wt%Ni, 0.08 wt%Co) and Fe-Ni phosphide (33.7 wt%Ni, 15.8 wt%P) in kamacite matrix of (6.7±0.2) wt%Ni and (0.39±0.02) wt%Co. In addition to the Fe-Ni phosphide lamellae, fine grains (several μm in mean diameter) of rhabdite are observed.

Allan Hills-77289: It has been reported in a previous paper (NAGATA *et al.*, 1983) that Allan Hills-77289 consists of taenite lamellae (59.0±1.4 wt%Fe, 39.5±1.6 wt%Ni) and granular Fe-Ni phosphide specks in kamacite matrix (92.7±0.1 wt%Fe, 6.83± 0.07 wt%Ni). Further metallographic studies have shown that the chemical composition of the kamacite matrix is given by (6.5–6.7) wt%Ni and (0.37–0.41) wt%Co, the composition of taenite lamellae by (29.6–34.8) wt%Ni and (0.08–0.09) wt%Co, and the composition of Fe-Ni phosphide by 37.7 wt%Ni, 0.07 wt%Co and 15.9 wt%P.

It may be suggested by the observed chemical and metallographical data that the ferromagnetic properties of Yamato-790517 and -790724 and Allan Hills-77263 and -77289 are mostly due to the dominant presence of kamacite phase, modified more or less by the co-existing taenite lamellae and specks, while those of Yamato-791694 are mostly due to the dominant presence of taenite phase, modified by the co-existing kamacite specks. On the other hand, the magnetic properties of Yamato-791076 will be considerably complicated, because of its widely spread plessitic structure. Since the bulk Ni content in Yamato-791076 is 13.60 wt%Ni while the average Ni contents in kamacite and taenite components are 6.1 and 29.7 wt%Ni respectively, an approximate weight ratio of kamacite to taenite is estimated as 68 to 32%. It will be expected then that the kamacite phase is dominant in the ferromagnetic properties at room temperature and higher temperatures of this iron meteorite, because Curie point is approximately 0°C for taenite of 30 wt%Ni (CRANGLE and HALLAM, 1963) and the amount of taenite component is definitely smaller than that of kamacite component. However, the magnetic properties of plessite phase comprising kamacite and taenite components may be not a simple superposition of those of independent kamacite and taenite phases. This point will have to be magnetically examined in some detail.

All the six iron meteorite examined in the present study contain Fe-Ni phosphides which are ferromagnetic. Except Yamato-790517, the P content in Fe-Ni phosphide grains in all the other five Antarctic iron meteorites is almost constant, being (15.80 ±0.11) wt% on average, regardless of their Ni content which ranges from 29 to 44 wt% in individual grains as shown in Fig. 1. The kamacite components of (5.0–8.5) wt%Ni in these iron meteorites also contain phosphorus of (0.025–0.12) wt%P in content, while the taenite components of (21–40) wt%Ni in them contain phosphorus of much smaller amount, namely, (0.000–0.025) wt%P. In the cases of coarse octahedrites, therefore, it can be approximately assumed that phosphorus is practically distributed into the kamacite phase which occupies almost the whole octahedrite and the Fe-Ni phosphide phase which contains 15.8 wt%P. Namely,

$$(\text{Bulk P content}) \simeq (\text{P content in kamacite}) + 15.8q$$

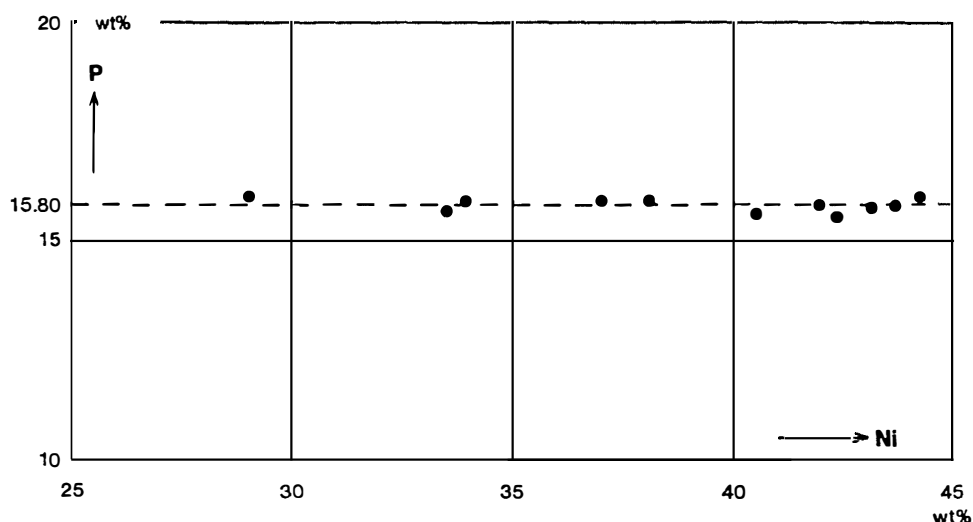in unit of weight percent, where q denotes the weight content of Fe-Ni phosphide.

Fig. 1. Phosphorus content vs. nickel content in (Fe, Ni)₃P grains in Antarctic iron meteorites.

In the cases of Ni-rich ataxites such as Yamato-791076 and -791694, the weight contents of kamacite (q_k) and taenite (q_t) can be approximately evaluated on an assumption that nickel is mostly distributed into kamacite and taenite phases; namely,

(Bulk Ni content)$\simeq$(Ni content in kamacite)$\times q_k+$(Ni content in taenite)$\times q_t$,

where $q_k+q_t\simeq1$. Then, the bulk content of phosphide in the Ni-rich ataxite will be approximately given by

(Bulk P content)$\simeq$(P content in kamacite)$\times q_k+$(P content in taenite)$\times q_t+15.8q$.

The contents (q) of Fe-Ni phosphide in the individual Antarctic iron meteorites thus evaluated are summarized in Table 1.

Although the chemical compositions of Fe-Ni phosphides in the five Antarctic iron meteorites are reasonably close to (Fe, Ni)₃P which also is ferromagnetic (GAMBINO *et al.*, 1967), the P content in Fe-Ni phosphide grains in Yamato-790517 is much smaller than 15.8 wt%P which can form the (Fe, Ni)₃P structure together with Fe and Ni as the remainder components. It seems likely that the Fe-Ni phosphide grains in Yamato-790517 are in the midst of forming rhabdite or schreibersite specks from the precipitated phospharus because of rapid cooling. The P content in kamacite matrix (0.24 wt%P) suggests that the quenching temperature for this Ni-poor ataxite is about 500°C in the solvus of P for kamacite (REED, 1966). For comparison, the P content in kamacite phases of all the other five iron meteorites examined in the present study is less than 0.12 wt%.

3. Magnetic Analysis

3.1. Magnetic hysteresis characteristics

The magnetic hysteresis curves at room temperature (22–26°C) are measured in a magnetic field range of -16 kOe ~16 kOe. The characteristic parameters such as

Table 2. Basic magnetic parameters of new Antarctic iron meteorites.

Magnetic parameter	Yamato-				Allan Hills-	
	790517	790724	791076	791694	77263	77289
I_s(emu/g)	207	204	192	138	207	201
I_R(emu/g)	0.35	0.45	1.55	0.65	0.66	0.07
H_c(Oe)	4.0	5.5	15.0	8.0	2.0	2.0
H_{RC}(Oe)	125	110	290	170	80	75
Θ_c (°C)	—	—	—	300–400	—	—
$\Theta^*_{\alpha \to \gamma}$(I)(°C)	750	730	740	740	755	750
(II)(°C)	760	725	725	—	755	750
$\Theta^*_{\gamma \to \alpha}$(I)(°C)	620,(455)	600	(590),450	—	615	615
(II)(°C)	625,(450)	600	(590),445	—	620	615

I_s:	Saturation magnetization	Θ_c:	Curie point
I_R:	Saturated remanent magnetization	$\Theta^*_{\alpha \to \gamma}$:	$\alpha \to \gamma$ transition temperature
H_c:	Coercive force	$\Theta^*_{\gamma \to \alpha}$:	$\gamma \to \alpha$ transition temperature
H_{RC}:	Remanence coercive force	(I):	First-run measurement
		(II):	Second-run measurement

saturation magnetization (I_s), saturated remanent magnetization (I_R), coercive force (H_c), and remanence coercive force (H_{RC}) of individual iron meteorites are summarized in Table 2.

The observed apparent values of I_R in the table are not the true values of I_R, because the demagnetization field effect dependent on the sample dimensions is not corrected. Hence, only the relative magnitude of I_R among individual samples can be taken into consideration. Apparent values of H_{RC} in the table also should be interpreted in the same way. It is obvious that the true value of I_R is much larger than the observed apparent value of I_R, while the true value of H_{RC} is much smaller than the observed apparent value of H_{RC}. However, the observed values of I_s and H_c can sufficiently well present their respective true values.

The I_s values larger than 200 emu/g and smaller than 210 emu/g at room temperature reasonably well represent kamacite phase containing a small amount of taenite in the Fe-Ni binary system (CRANGLE and HALLAM, 1963). The I_s values of Yamato-790517 and -790724 and Allan Hills-77263 and -77289, therefore, suggest that these iron meteorites are octahedrite or Ni-poor ataxite. On the other hand, the I_s value of Yamato-791694 (i.e. $I_s=138$ emu/g) suggests that the largest parts of this iron meteorite should be of taenite phase, because I_s values smaller than 170 emu/g at room temperature can be taken only by the f.c.c. taenite phase in the Fe-Ni binary system (CRANGLE and HALLAM, 1963). If we assume that the whole system of Yamato-791694 is occupied by a single taenite phase, its Ni content is estimated from the I_s vs. Ni content relation for taenite phase to be about 34 wt%Ni, which is in approximate agreement with the bulk Ni content. The I_s value of Yamato-791076 (i.e. $I_s=192$ emu/g) may suggest that this iron meteorite consists of larger parts of kamacite and the remaining smaller but considerable parts of taenite.

Coercive force of small value (i.e. $H_c=2$ Oe) of Allan Hills-77263 and -77289 suggests that these iron meteorites contain only a small portion of taenite lamellae in comparison with Yamao-790517 and -790724, the H_c values of which are 4.0 and 5.5 Oe

respectively. The relatively large H_c value of Yamato-791076 (*i.e.* $H_c=15$ Oe) suggests that metallographical structures comprising kamacite and taenite phases in this iron meteorite are considerably fine and complex, resulting in the mechanical stress and shape anisotropies. An intermediate value of H_c (*i.e.* $H_c=8$ Oe) of Yamato-791694 suggests that taenite matrix of this iron meteorite is not homogeneous but heterogeneously includes kamacite specks or lamellae.

3.2. Thermomagnetic characteristics

The thermomagnetic curves of the six Antarctic iron meteorites are measured in 10^{-5} Torr vacuum in a magnetic field of 10 kOe by a vibration magnetometer. The observed data of thermomagnetic parameters such as Curie point (Θ_c) of taenite component, $\alpha \rightarrow \gamma$ transition temperature of kamacite component in the heating process ($\Theta^*_{\alpha \rightarrow \gamma}$) and $\gamma \rightarrow \alpha$ transition temperature of kamacite component in the cooling process ($\Theta^*_{\gamma \rightarrow \alpha}$) are summarized in Table 2. The observed difference of the second-run ther-
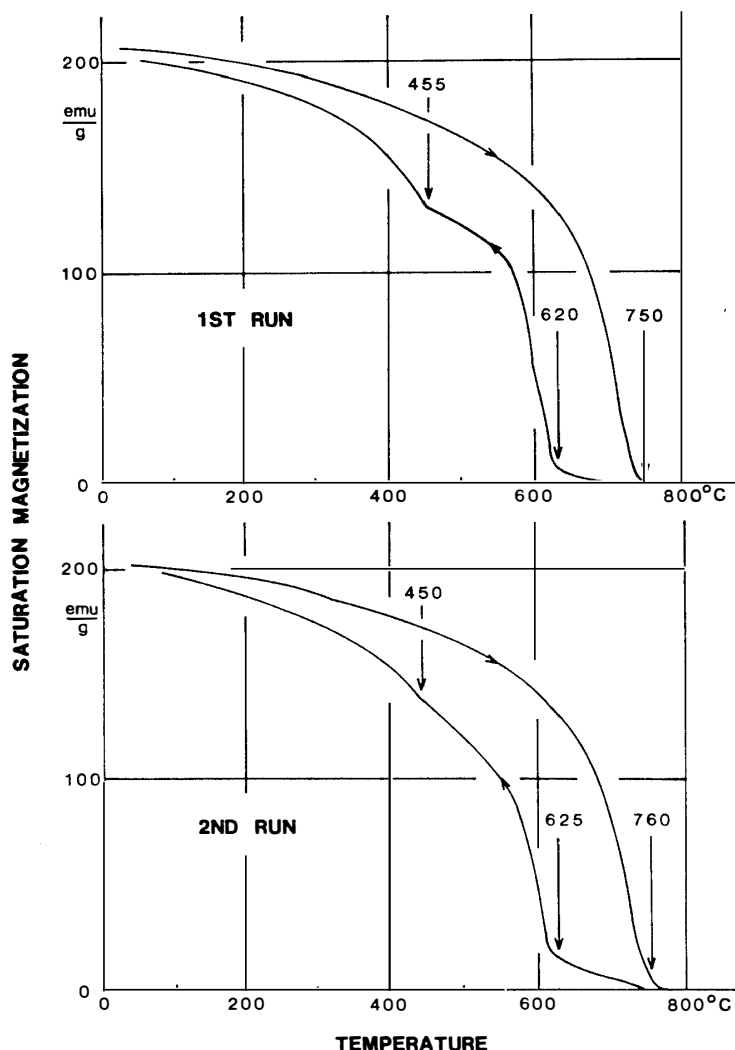

Fig. 2. First-run and second-run thermomagnetic curves of Yamato-790517 ($H_{ex}=10$ kOe).

momagnetic curves from the first-run thermomagnetic curves of individual samples, if any, will suggest the stability of identified magnetic phases against the heat treatment within the applied temperature range.

Yamato-790517 (Fig. 2): A magnetic phase represented by $\Theta^*_{\alpha\to\gamma}=750-760°C$ and $\Theta^*_{\gamma\to\alpha}=620-625°C$ is identified to a kamacite phase of 6.3–6.4 wt%Ni which forms the major matrix of Yamato-790517. In the first-run cooling thermomagnetic curve, a definite folding point, indicating a magnetic transition, is observed at about 455°C and the magnetic transition phenomenon is noticeably reduced in the second-run cooling thermomagnetic curve, whereas a Ni-poor kamacite phase of $\Theta^*_{\gamma\to\alpha}=720°C$ newly appears in the second-run cooling curve. The magnetic transition phenomenon at 450–455°C in the cooling process may be provisionally interpreted as due to the presence of an unequilibrated Ni-rich kamacite of about 12 wt%Ni, which is decomposed by the repeated heatings into the Ni-poorer kamacite phase of about 4 wt%Ni and taenite phases of 25 wt% or less in Ni content, Curie points of which are lower than
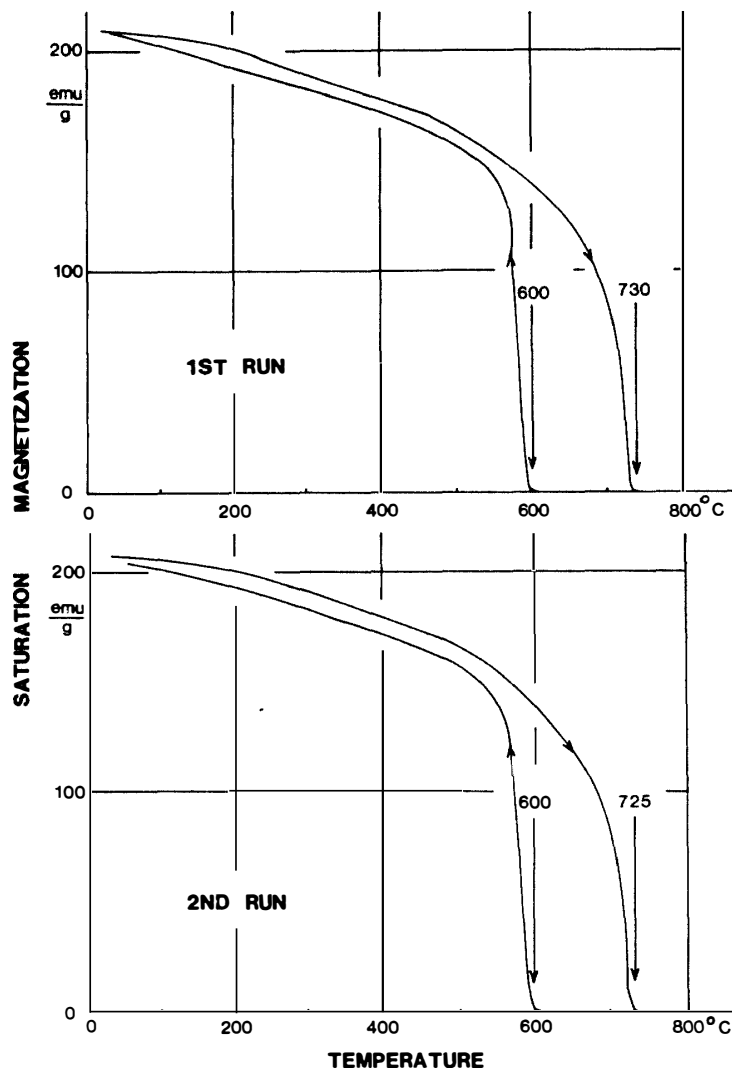

Fig. 3. First-run and second-run thermomagnetic curves of Yamato-790724 ($H_{ex}=10$ kOe).

0°C. Comparing these data of magnetic analysis with those of the microprobe analysis for Yamato-790517, the observed value of $\Theta^*_{\gamma\to\alpha}$ for the major kamacite phase (620–625°C) is a little too high to represent the kamacite matrix of (7.0 ± 0.1) wt%Ni in the Fe-Ni binary system. A possible effect of increasing the $\Theta^*_{\gamma\to\alpha}$ temperature by adding a relatively large amount of phosphorus may be involved in the present case, as indicated by the Fe-Ni-P equilibrium diagram (GOLDSTEIN and DOAN, 1972). The magnetic component responsible for the magnetic transition at about 450°C in the cooling process will be the P-poor Fe-Ni phosphide grains of (13.2 ± 1.6) wt%Ni and (0.75 ± 0.22) wt%P, which are relatively abundant as the fine grain in the kamacite matrix. However, the co-existence of Ni-rich kamacite grains of (18–24) wt%Ni and (0.3 ± 0.1) wt%P also may have to be taken into account.

Yamato-790724 (Fig. 3): The major magnetic component is a kamacite matrix of 7.0 wt%Ni which is represented by $\Theta^*_{\alpha\to\gamma}=730°C$ and $\Theta^*_{\gamma\to\alpha}=600°C$ in Fig. 3. As the magnetic transitions at both $\Theta^*_{\alpha\to\gamma}$ and $\Theta^*_{\gamma\to\alpha}$ are sufficiently sharp, the chemical
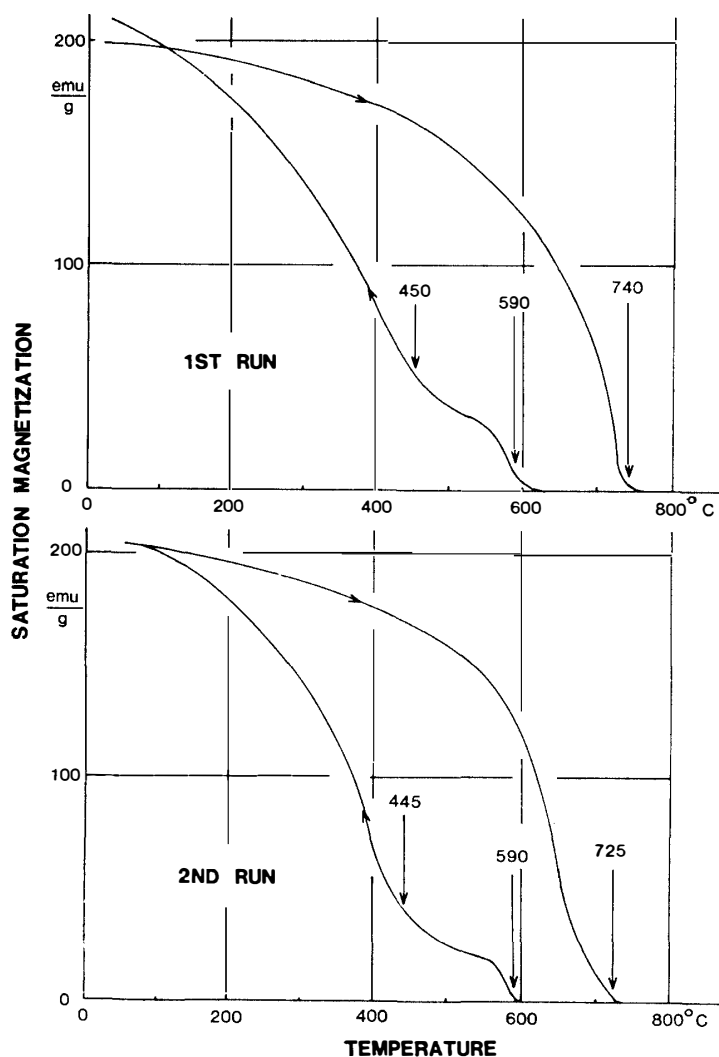

Fig. 4. First-run and second-run thermomagnetic curves of Yamato-791076 $(H_{ex}=10\ kOe)$.

composition of the kamacite matrix will be sharply concentrated around 7.0 wt%Ni. This magnetically analyzed value of Ni content in kamacite component is in good agreement with the Ni content value directly measured by the microprobe analyzer (*i.e.* 7.00 wt%Ni).

Yamato-791076 (Fig. 4): The major magnetic components of Yamato-791076 are a kamacite phase represented by $\Theta^*_{\gamma \to \alpha} = 590°C$ on average and an unequilibrated kamacite phase, the $\Theta^*_{\gamma \to \alpha}$ value of which continuously distribute around 450°C. The kamacite phase of $\Theta^*_{\gamma \to \alpha} = 590°C$, which corresponds to 7.3 wt%Ni kamacite, may be identified to the spindle-shape bands of kamacite of 7.0 wt%Ni which fill up the gaps between the microplessitic net systems. The folding of thermomagnetic curve around 450°C still persists in the second-run measurement and no trace of a magnetic transition can be observed around 450°C in the heating thermomagnetic curve, so that the magnetic transition around 450°C in the cooling thermomagnetic curve may be identified to the $\gamma \to \alpha$ transition of an unequilibrated Ni-rich kamacite phase of about 12 wt%Ni. However, this simple magnetic analysis interpretation can not be directly supported by the result of microprobe analysis of the metallographic structure, which is mostly represented by the kamacite bands of spindle shape and the net plessites consisting of taenite nets (21.5–36.5 wt%Ni) and included minute specks (smaller than 10 μm in mean diameter) of kamacite (5.1 wt%Ni). It seems likely, therefore, that plessite nets magnetically behave as an unequilibrated Ni-rich kamacite phase whose chemical composition is near the average composition of plessite nets.

A similar magnetic phenomenon has already been observed for Allan Hills-77255 ataxite of 12.2 wt%Ni in its bulk chemical composition (FISHER *et al.*, 1980). The metallographic structure of Allan Hills-77255 is represented by a large number of kamacite spindle of 20 μm × 120 μm in dimensions dispersed in the microplessitic matrix. Its thermomagnetic characteristics, however, are represented by a single thermomagnetic cycle curve of Ni-rich kamacite of $\Theta^*_{\alpha \to \gamma} = 760°C$ and $\Theta^*_{\gamma \to \alpha} = 500–585°C$ in the first-run measurements and $\Theta^*_{\alpha \to \gamma} = 735°C$ and $\Theta^*_{\gamma \to \alpha} = 450–550°C$ in the second-run measurements (Fig. 5). Thus, the metallographic constitution comprising kamacite spindles and α- and γ-phases of microplessite is not exactly reflected on the observed thermomagnetic curves in the case of Allan Hills-77255. Instead, the thermomagnetic curves apparently indicate that almost the whole of this ataxite magnetically behaves as a single unequilibrated Ni-rich kamacite phase of (7.5–10.0) wt%Ni in the first-run measurement and as that of (8.5–12.0) wt%Ni in the second-run measurement.

In the present case of Yamato-791076, the presence of spindle-shape kamacite phase is clearly shown as a magnetic component of $\Theta^*_{\gamma \to \alpha} = 590°C$ of the thermomagnetic curve, whereas that of kamacite spindles is not separately observed in the thermomagnetic curves of Allan Hills-77255. It seems likely thus that the thermomagnetic characteristics of plessitic structure in regard to the $\alpha \to \gamma$ transition in a heating process and the $\gamma \to \alpha$ transition in a cooling process are subject to a sort of cooperative phenomenon among neighboring kamacite and taenite phases which couple with each other within a certain mutual distance. Since the spindle-shape kamacites of (40–80 μm) × (200–500 μm) in dimensions in microplessitic matrix in Yamato-791076 are separately detected on its thermomagnetic curve, whereas the kamacite spindles of 20 μm × 120 μm in dimensions in Allan Hills-77255 are not detectable on its thermomagnetic curves,
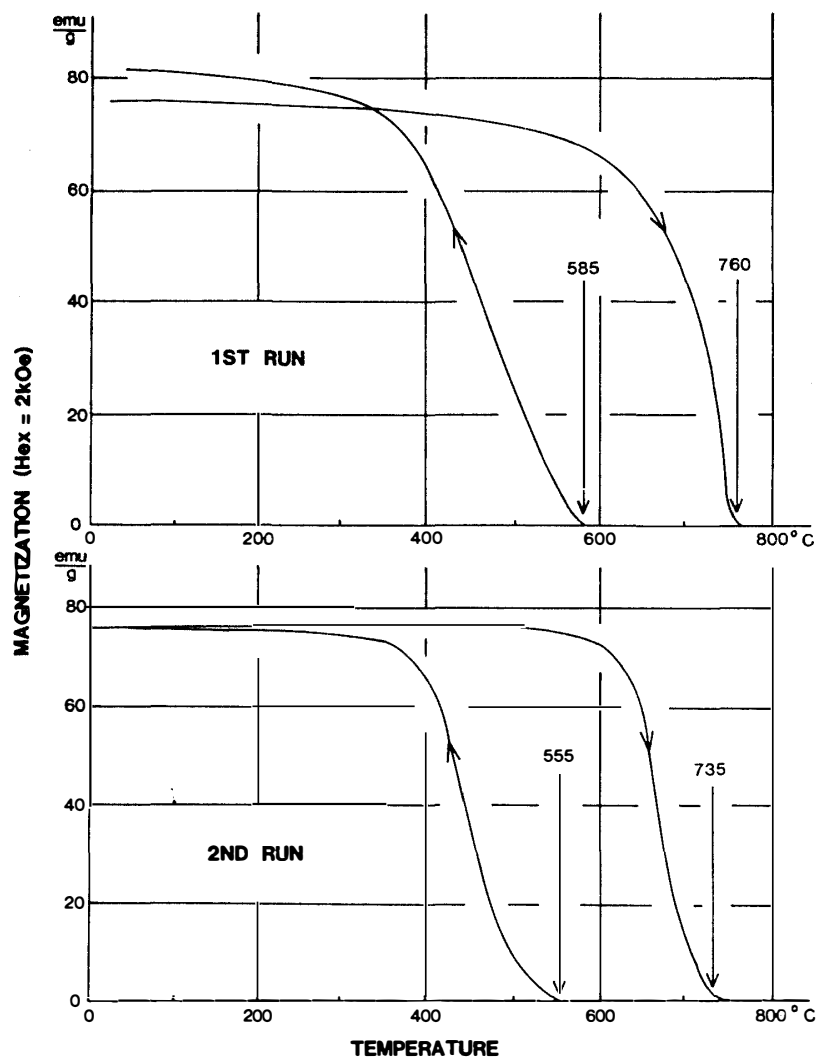
*Fig. 5.   First-run and second-run thermomagnetic curves of Allan Hills-77255
(Hex =2 kOe).*

the assumed critical dimensions of kamacite spindles or bands for the cooperative coupling with the microplessitic matrix will be about 30 μm × 150 μm in kamacite spindle dimensions or about 30 μm in kamacite band width.

If this assumption of a cooperative transition of a plessite structure from γ-phase to α-phase in a cooling process is accepted, the magnetically observed transition around 450°C of an apparent unequilibrated Ni-rich kamacite phase of Yamato-791076 can be interpreted as the $\gamma\rightarrow\alpha$ transition of the net plessite.

Yamato-791694 (Fig. 6):   The cooling thermomagnetic curve of the first-run and both the heating and cooling thermomagnetic curves of the second-run of Yamato-791694 indicate that its largest parts are taenite of Θ_c=300–400°C, while the heating thermomagnetic curve of the first-run indicates that a magnetization of a kamacite component of $\Theta^*_{\alpha\rightarrow\gamma}\simeq$740°C is present in the initial state and is additively superposed on the heating thermomagnetic curve of taenite component. The kamacite magnetic component may probably represent kamacite specks of 6.8 wt%Ni which are dispersed
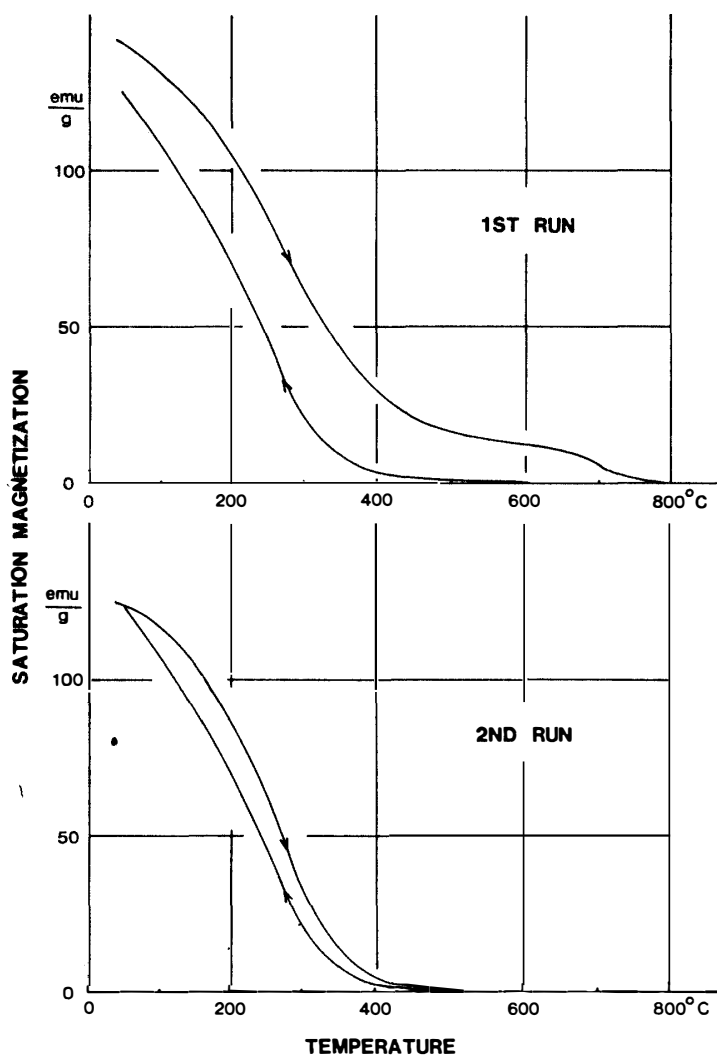
Fig. 6.   First-run and second-run thermomagnetic curves of Yamato-
791694 $(H_{ex}=10\ kOe)$.

in taenite matrix.   By heating up to about 800°C, however, the kamacite specks appear
to be mostly dissolved into the taenite matrix.

According to Fe-Ni alloy Curie point data (CRANGLE and HALLAM, 1963), Curie
point of taenite at 300 and 400°C correspond to 38 and 43 wt%Ni respectively of the
f.c.c. Fe-Ni alloy metal.   On the other hand, the bulk Ni content of Yamato-791694
is 35.50 wt% and the directly measured value of Ni content in its taenite matrix is (35.5
±0.4) wt%Ni.   Then, the average value of Ni content in taenite estimated by the pres-
ent magnetic analysis (i.e. about 40 wt%Ni) is larger than the directly measured Ni
content value by about 5 wt%.   The considerable difference between the magnetic and
microprobe analysis data will have to be examined in more detail in the future.

Allan Hills-77263 (Fig. 7):   The magnetic component is almost a kamacite phase
of 6.4–6.6 wt%Ni which is represented by $\Theta^{*}_{\alpha\rightarrow\gamma}=755°C$ and $\Theta^{*}_{\gamma\rightarrow\alpha}=615$–620°C.   This
result is in agreement with the microprobe analysis data that this coarse octahedrite
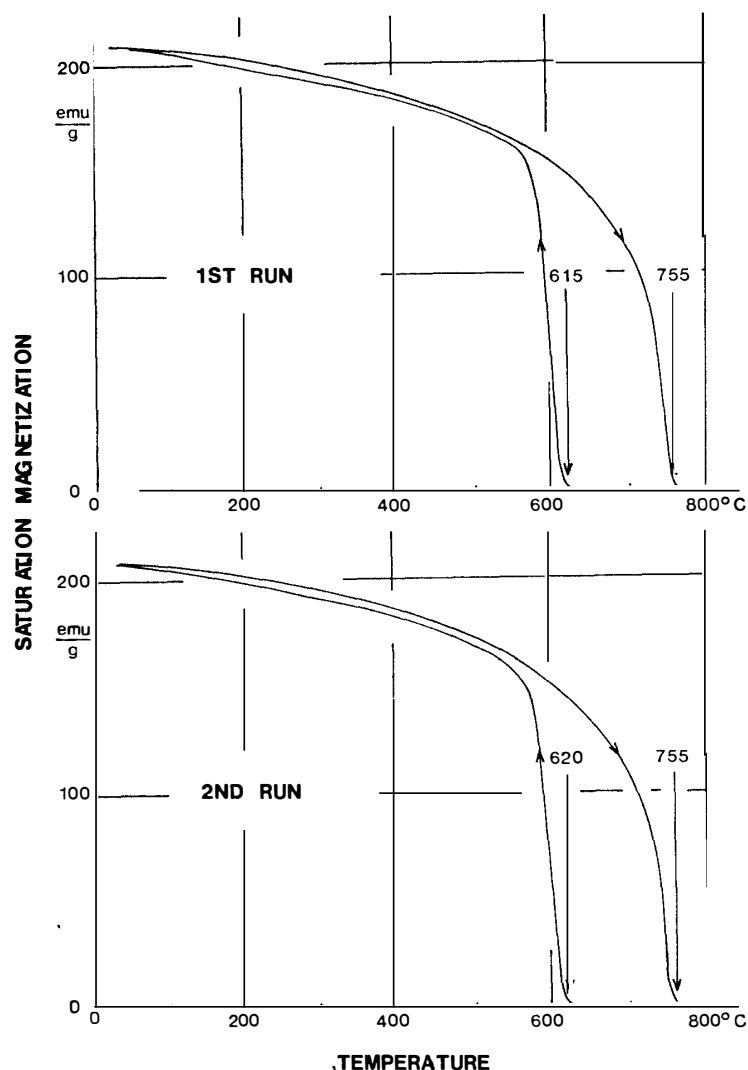is mostly occupied by kamacite matrix of (6.7±0.2) wt%Ni and (0.39±0.02) wt%Co.

Fig. 7. First-run and second-run thermomagnetic curves of Allan Hills-77263 ($H_{ex}=10\ kOe$).

Allan Hills-77289 (Fig. 8): The magnetic component is almost a kamacite phase of 6.4 wt%Ni represented by $\Theta^*_{\alpha\to\gamma}=750°C$ and $\Theta^*_{\gamma\to\alpha}=615°C$. The thermomagnetic characteristics of this coarse octahedrite are almost same as those of Allan Hills-77263 just as former's chemical and metallographic compositions are very similar to those of the latter. It seems very likely, therefore, that these two coarse octahedrites are fragments of a single octahedrite mass.

4. Magnetic Behaviors of Minor Components

LOVERING and PARRY (1962) have pointed out a possibility to magnetically estimate small amounts of taenite and schreibersite which co-exist with kamacite matrix in iron meteorites by analyzing their thermomagnetic curves. Figure 9 shows enlarged first-run heating thermomagnetic curves of Yamato-790517 and -790724 for example. A magnetic transition at 270°C in Yamato-790724 may indicate Curie point of taenite or
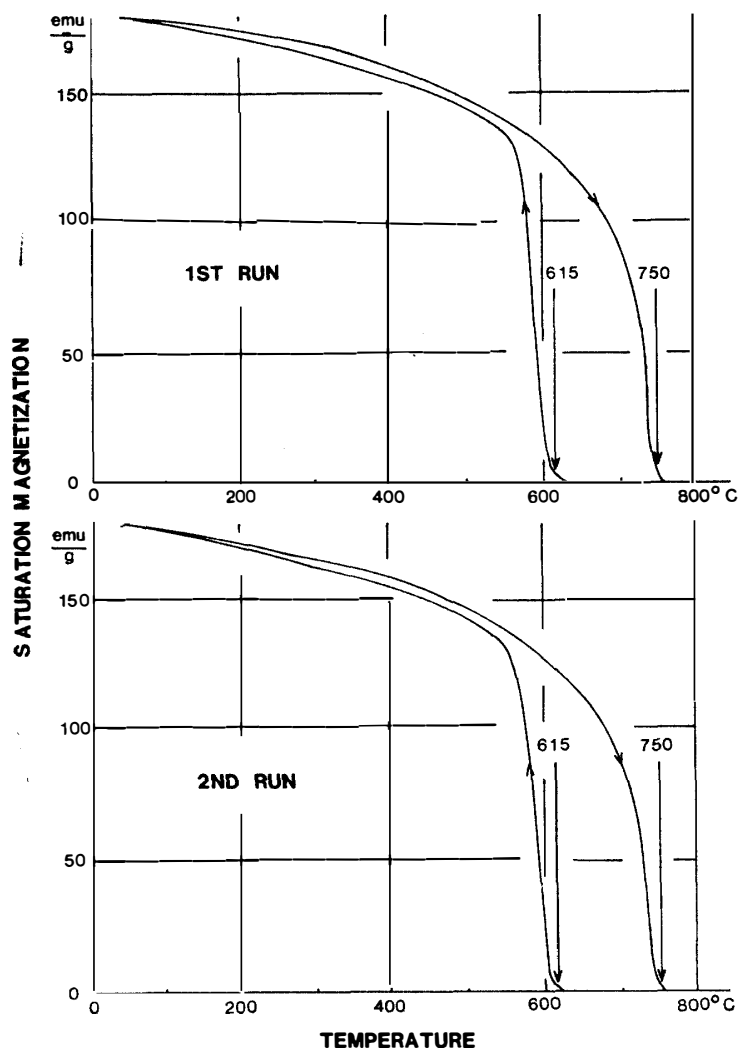
Fig. 8.   First-run and second-run thermomagnetic curves
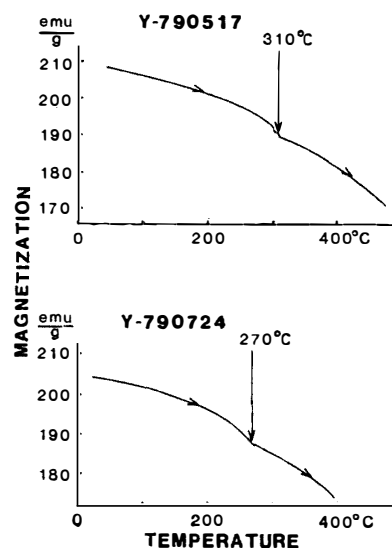of Allan Hills-77289 ($H_{ex}=10$ kOe).

Fig. 9.   Englarged first-run heating thermomagnetic curves of
Yamato-790517 and -790724.

Fe-Ni phosphide phase.   If the small additional magnetic component (about 3 emu/g
in I_s) is assumed to be taenite, the Ni content in the taenite phase is estimated as 37
wt%Ni on the basis of Crangle-Hallam's Curie point vs. Ni content data for Fe-Ni
alloys (CRANGLE and HALLAM, 1963) or as 34 wt%Ni on the basis of Hoselitz's data
(HOSELITZ, 1952).   If alternatively the additional magnetic component assumes schrei-
bersite (Fe, Ni)$_3$P, then, the Ni content is estimated to be about 20 wt%Ni on the
basis of an experimentally measured relationship between Curie point and Ni content
for (Fe, Ni)$_3$P (GAMBINO et al., 1967).

In the microprobe analysis data of Yamato-790724, on the other band, the content
of schreibersite is negligibly small (0.04 wt%) and the measured average Ni content in
the schreibersite specks is 29 wt%Ni.   It seems most likely therefore that the magnet-
ically observed additional magnetic component is identified to the taenite specks of
(28–33) wt%Ni detected by the microprobe analysis.   Since the content of Fe-Ni

phosphide is negligibly small, the observed difference between the bulk Ni content (7.46 wt%) and the Ni content in kamacite matrix (7.00 wt%) can be approximately assumed to be due to the coexistence of the taenite component in Yamato-790724. If the most probable average value of Ni content in taenite is 34 wt%, then, the content of taenite is estimated to be 1.7 wt%. As the saturation magnetization moment of 34 wt%Ni taenite is 140 emu/g at 20°C (CRANGLE and HALLAM, 1963), the saturation magnetization of taenite component in Yamato-790724 is evaluated to be 2.4 emu/g, which is in approximate agreement with the magnetically observed value. If alternatively the average taenite Ni content assumes 37 wt%, the taenite content and its saturation magnetization moment are estimated as 1.53 wt% and 2.5 emu/g respectively. From the thermomagnetic curve alone, however, there is no way at present to distinguish between taenite and schreibersite.

As for the observed additional magnetic component of 310°C in magnetic transition temperature and about 5 emu/g in saturation magnetization moment for Yamato-790517 (Fig. 9), it could be presumed that the magnetic component can be identified either to a taenite component of 39 wt%Ni (Crangle and Hallam model) or 36 wt%Ni (Hoselitz model) or to a schreibersite component of 15 wt%Ni. If it is a taenite component, its content is magnetically estimated to be about 3.0 wt%. If alternatively it is assumed to be schreibersite, its content is magnetically evaluated as about 3.8 wt%. However, the results of microprobe analysis have shown no evidence of the presence of taenite component of larger than 30 wt% in Ni content nor that of schreibersite in Yamato-790517. Further, the additional small magnetic component observed in the first-run heating thermomagnetic curve almost completely disappears in the second-run heating curve. It appears that the additional magnetic component, which is thermally unstable, may represent either the P-rich Fe-Ni phosphide grains or the Ni-rich kamacite grains, but the magnetic properties of these magnetic materials have not yet been known. In brief, the additional magnetic component in Yamato-790517 may not be reliably identified to a certain definite magnetic mineral at the present stage.

In both Allan Hills-77263 and -77289, Ni content in kamacite matrix is close to that in their bulk composition, suggesting that the contents of taenite and schreibersite in these iron meteorites are very small. The probable contents of (Fe, Ni)$_3$P component in these iron meteorites are given in Table 1. The saturation magnetic moment and Curie point of schreibersite component thus estimated from the chemical composition are 0.23 emu/g and 140°C respectively for Allan Hills-77263 and 0.23 emu/g and 105°C respectively for Allan Hills-77289. These additional magnetic moments of schreibersite component may be too small to be detected on the thermomagnetic curves shown in Figs. 7 and 8.

As already discussed in the preceding section, the magnetic behaviors of thermomagnetic curves of the major magnetic components in Yamato-791076 and -791694 are fairly complex so that it will be difficult to deal with possible magnetic behaviors of the minor magnetic component such as schreibersite on the basis of their ordinary thermomagnetic curves.

5. Concluding Remarks

In the present work, the magnetic hysteresis curves at room temperature and the thermomagnetic curves of 6 new Antarctic iron meteorites are analyzed in comparison with their respective metallographic structures and chemical compositions.

The $I_s(\alpha)/I_s$ values of Yamato-790517 and Allan Hills-77263 and -77289 are almost the unity and their $\Theta^*_{\gamma\to\alpha}$ values range between 600 and 625°C, whence these three Antarctic iron meteorites certainly belong to the octahedrite group in the magnetic classification scheme (NAGATA, 1982). As the $I_s(\alpha)/I_s$ value is nearly zero and Θ_c in the cooling thermomagnetic curve is 300–400°C for Yamato-791694, this iron meteorite certainly belongs to the group of Ni-rich ataxite in the magnetic classification scheme. The thermomagnetic curves of Yamato-790517 are a little more complex than those of the three new Antarctic octahedrites, consisting of a main kamacite phase of $\Theta^*_{\gamma\to\alpha} = 620$–625°C and two other magnetic phases represented by $\Theta^*_{\gamma\to\alpha} = 450$–455°C and $\Theta^*_{\gamma\to\alpha} \simeq 720$°C. In comparison of these magnetic data with the microprobe analysis data of metallographic structure and chemical composition, it seems most likely that the second magnetic phase of $\Theta^*_{\gamma\to\alpha} = 450$–455°C is identified to small granular grains of Ni- and P-rich kamacite of 13 wt%Ni and 0.75 wt%P, which are dispersed in kamacite matrix. Yamato-790517 can therefore be classified into the group of Ni-poor ataxite. The small magnetic grains in this Ni-poor ataxite are thermally unstable as shown in Fig. 2 even in laboratory time scale. Further studies in detail on magnetic properties of this kind of iron meteorite will be required in the future.

The thermomagnetic curves of Yamato-791076 consisting of the major magnetic component of Ni-rich kamacite of about 12 wt%Ni and the secondary magnetic component of kamacite of about 7 wt%Ni may suggest that this iron meteorite is a finest octahedrite or a Ni-rich ataxite containing a relatively poor amount of nickel. The microprobe analysis data show, however, that the apparent Ni-rich kamacite phase represents a plessite phase consisting of taenite nets of 30 wt%Ni on average and kamacite of about 5 wt%Ni fulfilling the mesh space of the taenite nets. The magnetic behaviors of such a plessitic structure have not yet been well known. This problem also will have to be studied in more detail.

References

CRANGLE, J. and HALLAM, G. C. (1963): The magnetization of face-centered cubic and body-centered cubic iron-nickel alloys. Proc. R. Soc. London, Ser. A, 255, 509–519.

FISHER, R. M., SPANGLER, C. E., Jr. and NAGATA, T. (1978): Metallographic properties of Yamato iron meteorite, Yamato-75031 and a stony-iron meteorite, Yamato-74044. Mem. Natl Inst. Polar Res., Spec. Issue, 8, 248–259.

FISHER, R. M., SPANGLER, C. E., Jr., NAGATA, T. and FUNAKI, M. (1979): Metallographic and magnetic properties of Allan Hills 762 iron meteorite. Mem. Natl Inst. Polar Res., Spec. Issue, 12, 270–282.

FISHER, R. M., SZIRMAE, A. and NAGATA, T. (1980): Metallographic and magnetic properties of Allan Hills A77255, Derrik Peak A78003 and A78007, and Russian meteorite Sikhote-Alin. Mem. Natl Inst. Polar Res., Spec. Issue, 17, 276–290.

GAMBINO, R. J., McGUIRE, T. R. and NAKAMURA, Y. (1967): Magnetic properties of the iron group metal phosphides. J. Appl. Phys., 38 (3), 1253–1255.

GOLDSTEIN, J. I. and DOAN, A. S., Jr. (1972): The effect of phosphorus on the formation of the Widemanstätten pattern in iron meteorites. Geochim. Cosmochim. Acta, **36**, 51–69.

GUS'KOVA, Ye. G. (1972): Magnitnye Svoystva Meteorytov (The Magnetic Properties of Meteorites). Leningrad, Nauka, 107 p. (English translation NASA TT F-792, 1976, 143 p.).

HOSELITZ, K. (1952): Ferromagnetic Properties of Metals and Alloys. Oxford, Clarendon, 317 p.

LOVERING, J. F. and PARRY, L. G. (1962): Thermomagnetic analysis of co-existing nickel-iron metal phases in iron meteorites and the thermal histories of meteorites. Geochim. Cosmochim. Acta, **26**, 361–382.

NAGATA, T. (1978): Magnetic properties of an iron meteorite (Yamato-75031) and a pallasite (Yamato-74044). Mem. Natl Inst. Polar Res., Spec. Issue, **8**, 240–248.

NAGATA, T. (1982): Magnetic classification of meteorites (V); Iron meteorites. Mem. Natl Inst. Polar Res., Spec. Issue, **25**, 216–221.

NAGATA, T., FISHER, R. M. and SUGIURA, N. (1976): Metallographic and magnetic properties of a Yamato iron meteorite–Yamato-75105. Mem. Natl Inst. Polar Res., Ser. C (Earth Sci.), **10**, 1–11.

NAGATA, T., MASUDA, A. and TAGUCHI, I. (1983): Chemical studies of the Antarctic iron meteorites; Yamato-790724, ALH-77263 and ALH-77289. Mem. Natl Inst. Polar Res., Spec. Issue, **30**, 237–246.

REED, S. J. B. (1966): Electron-probe microanalysis of schreibersite and rhabdite in iron meteorites. Geochim. Cosmochim. Acta, **29**, 513–534.